AFRL-HE-BR-TR-2000-0118

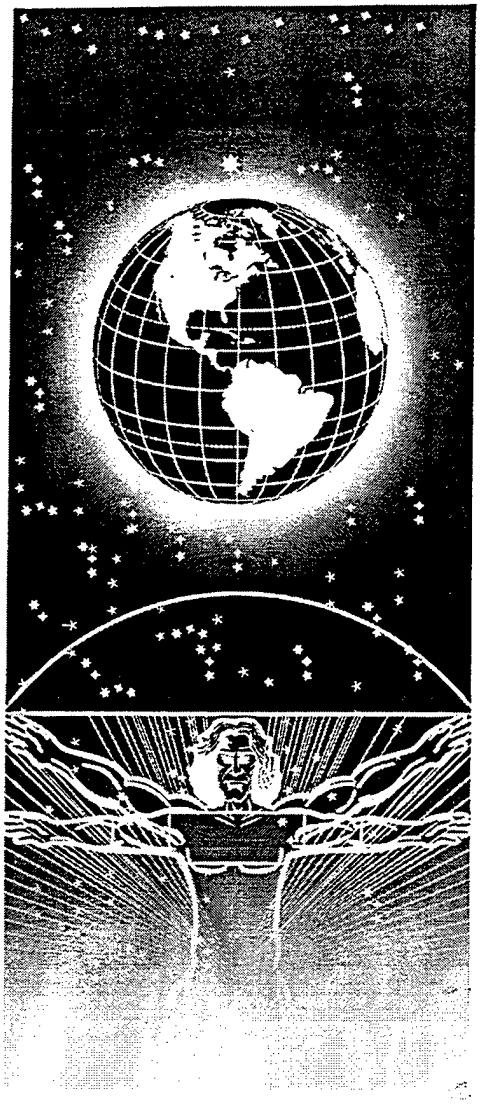

UNITED STATES AIR FORCE
RESEARCH LABORATORY

STATISTICAL ASPECTS OF OPTICAL OR MICROWAVE MEASUREMENTS OF MATERIAL PROPERTIES

Michael G. Block
Richard A. Albanese

HUMAN EFFECTIVENESS DIRECTORATE
DIRECTED ENERGY BIOEFFECTS DIVISION
BIOMECHANISMS AND MODELING BRANCH
2503 Gillingham Drive
Brooks AFB, Texas 78235-5102

September 2000

NOTICES

This report is published in the interest of scientific and technical information exchange and does not constitute approval or disapproval of its ideas or findings.

Using Government drawings, specifications, or other data included in this document for any purpose other than Government-related procurement does not in any way obligate the US Government. The fact that the Government formulated or supplied the drawings, specifications, or other data, does not license the holder or any other person or corporation, or convey any rights or permission to manufacture, use, or sell any patented invention that may relate to them.

The Office of Public Affairs has reviewed this report, and it is releasable to the National Technical Information Service, where it will be available to the general public, including foreign nationals.

This report has been reviewed and is approved for publication.

Michael G. Block OD

MICHAEL G. BLOCK
Project Scientist

RICHARD L. MILLER, Ph.D.
Chief, Directed Energy Bioeffects Division

REPORT DOCUMENTATION PAGE

Form Approved
OMB No. 0704-01-0188

PLEASE DO NOT RETURN YOUR FORM TO THE ABOVE ADDRESS.

1. REPORT DATE *(DD-MM-YYYY)*	2. REPORT TYPE	3. DATES COVERED *(From - To)*
01-09-2000	Final Report	Jun 97 - Sep 00

4. TITLE AND SUBTITLE
Statistical Aspects of Optical or Microwave Measurements of Material Properties

5a. CONTRACT NUMBER
F41622-96-D-0008

5b. GRANT NUMBER

5c. PROGRAM ELEMENT NUMBER
62202F

6. AUTHORS
Michael G. Block
Richard A. Albanese

5d. PROJECT NUMBER
7757

5e. TASK NUMBER
B4

5f. WORK UNIT NUMBER
10

7. PERFORMING ORGANIZATION NAME(S) AND ADDRESS(ES)
Air Force Research Laboratory (AFMC), Human Effectiveness Directorate
Directed Energy Bioeffects Division
Biomechanisms and Modeling Branch
2503 Gillingham Drive, Building 175E, Brooks AFB, Texas 78235-5102

8. PERFORMING ORGANIZATION REPORT NUMBER
AFRL-HE-BR-TR-2000-0118

9. SPONSORING/MONITORING AGENCY NAME(S) AND ADDRESS(ES)

10. SPONSOR/MONITOR'S ACRONYM(S)

11. SPONSOR/MONITOR'S REPORT NUMBER(S)

12. DISTRIBUTION/AVAILABILITY STATEMENT
Approved for public release; distribution unlimited

13. SUPPLEMENTARY NOTES

14. ABSTRACT
We seek a deeper understanding of the effect of noise on the measurement of material properties. We have found very few articles on the issue of measurement error associated with optical systems or antenna apertures that might be used to measure material properties. This report is an initial study of apertures and errors that may be associated with the use of apertures in the measurement of material properties. Bandwidth limited white noise generated by using the Rice algorithm is simulated in the aperture. Using a Legendre curve fitting technique, the diffraction pattern was smoothed and image resolution was enhanced. Since the diffraction pattern first minimum permits estimation of radiation frequency, the effect of input noise on the location of the first minimum of the diffraction pattern was evaluated.

15. SUBJECT TERMS
antenna apertures, optical systems, Rice algorithm, bandwidth limited white noise, measurement error, diffraction pattern, Fourier transform

16. SECURITY CLASSIFICATION OF:			17. LIMITATION OF ABSTRACT	18. NUMBER OF PAGES	19a. NAME OF RESPONSIBLE PERSON
a. REPORT	b. ABSTRACT	c. THIS PAGE			Michael G. Block
U	U	U	UU	21	19B. TELEPHONE NUMBER *(Include area code)* 210-536-2478

Statistical Aspects of Optical or Microwave Measurements of Material Properties
Michael G. Block and Richard A. Albanese

Introduction.

Many materials of importance to military or industrial applications have dielectric constants and conductivity values that are frequency dependent. These materials are therefore called dispersive since the phase velocity of electromagnetic radiation within the material is frequency dependent [1].

The *direct problem of electromagnetic scattering* involves being given the dielectric constant and conductivity of a material as a function of frequency and inferring from that data how an incident electromagnetic pulse or continuous wave propagates within the material. An *inverse problem of electromagnetic scattering* involves being given an incident and reflected electromagnetic pulse, or an adequate sequence of incident and reflected continuous waves, and inferring from these data the frequency dependent dielectric constant and conductivity of the material [2].

In the last ten to fifteen years there has been increased interest in the inverse problem described above. The possibility exists of radiating a surface from a great distance and receiving the reflected signal in return and from this pair inferring the material that constitutes the surface. For example, bodies of water could be interrogated to determine whether or not departures from certain standards of purity exist. An early study of this problem by Krueger and Beezely [3] showed that the surface material could indeed be determined from data on the incident and reflected pulse. However, these workers observed that the measurement of material conductivity was extremely sensitive to noise that is inevitable in real radiated or received signals. Using a different method, Albanese, Penn and Medina also showed an extreme sensitivity of the material conductivity estimate to noise [4].

We seek a deeper understanding of the effect of noise on the measurement of material properties. We have found very few articles on the issue of measurement error associated with optical systems or antenna apertures that might be used in the measurement of material properties. This report is an initial study of apertures and errors that may be associated with the use of apertures in the measurement of material properties.

Aperture nulls when the experimentalist knows aperture diameter provide estimates of the incoming frequency. Measuring diffraction pattern peaks provides estimates of incoming intensity at that frequency. A material is determined, for example, by its absorption of radiation at selected frequencies. Thus measurement of reflected

energy at given frequencies is important to material determination. In this report, we do not discuss the entire process of material determination, rather, we focus on frequency or wave length estimation.

Another use of this aperture study is toward an analysis of antennas that are uniformly excited. In this case we are looking at the stability of the beam structure in the face of fabrication errors.

Theory.

We consider the slit aperture treating the scalar case. We use Fraunhofer diffraction theory and compute the far field pattern $U(x_0)$ as a function of the aperture distribution $U(x_1)$ using the equation [5,6]

$$U(x_0) = \frac{e^{jkz} e^{j\frac{k}{2z}x_0^2}}{j\lambda z} \int_{-\infty}^{\infty} U(x_1) e^{-j\frac{2\pi}{\lambda z}x_0 x_1} dx_1$$

In the above equation $j = \sqrt{-1}$, z is the distance from the aperture to the target plane, λ is the wavelength of the radiation, x_1 is the distance across the aperture, and x_0 is distance across the target plane.

If we consider first, uniform excitation across an aperture of length l, we can use $U(x_1) = 1$ within the aperture. Doing this we find the following:

$$U(x_0) = \frac{e^{jkz} e^{j\frac{k}{2z}x_0^2}}{j\lambda z} \int_{-\infty}^{\infty} e^{-j\frac{2\pi}{\lambda z}x_0 x_1} dx_1 = \frac{e^{jkz} e^{j\frac{k}{2z}x_0^2}}{j\lambda z} \left[\frac{e^{-j\frac{2\pi}{\lambda z}x_0 x_1}}{-j\frac{2\pi}{\lambda z}x_0} \right]_{-l/2}^{l/2} = \frac{e^{jkz} e^{j\frac{k}{2z}x_0^2}}{j\lambda z} \left[\frac{\sin(\frac{\pi l}{\lambda z}x_0)}{\frac{\pi}{\lambda z}x_0} \right]$$

equation #2

We consider that the measured quantity in most experimental settings is the electromagnetic intensity $I(x_0)$ given by $|U(x_0)|^2$. That is, in many, if not most, experiments that we are aware of phase information is lost. Thus,

$$I(x_0) = \frac{l^2}{\lambda^2 z^2} \frac{\sin^2(\frac{\pi l}{\lambda z}x_0)}{(\frac{\pi l}{\lambda z}x_0)^2}$$

The above equation provides the intensity diffraction pattern. This equation has at least two interesting features.

First, notice that the distance to the first beam null is $x_{n,0}$ given by

$$\frac{x_{n,0}}{z} = \frac{\lambda}{l}$$

This equation says that the ratio of the effective illuminated area ($x_{n,0}$) to the distance to the target (z) equals the ratio of the wavelength (λ) to the aperture length (l). This is the famous "λ / l" constraint studied by Chu and others [7] and is also known as the diffraction limit. **This distance to the first null will be the object of our primary interest as it is a measure of incoming frequency and/or distance to the target.**

Second, notice that, in the equation for spot intensity, uncertainty in knowledge of the wavelength, and uncertainty or inaccuracy with respect to measurement of range to the target, enter into this equation multiplicatively, that is, as the product ($\lambda \cdot z$). If one considers λ and z as drawn from normal or Gaussian distributions, then the variance of the product will generally greatly exceed the variance of either random variable.

The height of the central peak in the diffraction curve, when there is no noise in the aperture, is

$$I(0) = \frac{l^2}{\lambda^2 z^2}$$

We will study the impact of transmission imperfections in the aperture as they relate to the far field pattern. To do this we will add low amplitude narrow band noise to the aperture transmission function. That is, we consider

$$U(x_1) = 1 + \eta(x_1)$$

In the above equation $\eta(x_1)$ is a narrow band stochastic process whose argument is the spatial variable x_1 that describes position within the aperture. We have used the Rice representation [8] for the narrow band stochastic process $\eta(x_1)$. That is, we use,

$$\eta(x_1) = \sum_{n=1}^{Bl} \left({}^k a_n \cos \omega_n x_1 + {}^k b_n \sin \omega_n x_1 \right)$$

In the above equation, as before, l is the size of the slit aperture under study. B is the bandwidth in spatial frequency (cycles per meter) of the noise process. The superscript k refers to a given stochastic realization, and each ${}^k a_n, {}^k b_m$ pair are uncorrelated for every

n and m. Similarly, each ${}^{k}a_n, {}^{k}a_m$ and ${}^{k}b_n, {}^{k}b_m$ pair is uncorrelated for every n and m. We have, following Bendat:

$$\omega_n = 2\pi f_n, \quad f_n = n\Delta f = \frac{n}{l}, \quad n = 1,2,3,...$$

The coefficients ${}^{k}a_n$ and ${}^{k}b_n$, with the correlation structure defined above, also have zero means, and are considered drawn from normal (Gaussian) distributions with variances that may be specific to the spatial frequency, namely:

$$\left\langle {}^{k}a_n^2 \right\rangle_{AV} = \left\langle {}^{k}b_n^2 \right\rangle_{AV} = \sigma_{f_n}^2 \Delta f$$

Now we will place the perturbed transmission function into the equation for Fraunhofer diffraction.

$$U(x_0) = \frac{e^{jkz} e^{j\frac{k}{2z}x_0^2}}{j\lambda z} \int_{-\infty}^{\infty} [1+\eta(x_1)] e^{-j\frac{2\pi}{\lambda z}x_0 x_1} dx_1 =$$

$$\frac{e^{jkz} e^{j\frac{k}{2z}x_0^2}}{j\lambda z} \int_{-\frac{l}{2}}^{\frac{l}{2}} e^{-j\frac{2\pi}{\lambda z}x_0 x_1} dx_1 + \frac{e^{jkz} e^{j\frac{k}{2z}x_0^2}}{j\lambda z} \sum_{n=1}^{Bl} \int_{-\frac{l}{2}}^{\frac{l}{2}} \left({}^{k}a_n \cos\omega_n x_1 + {}^{k}b_n \sin\omega_n x_1 \right) e^{-j\frac{2\pi}{\lambda z}x_0 x_1} dx_1$$

We simplify this last equation using Euler's equation and previous results as outlined below.

$$({}^{k}a_n \cos\omega_n x_1 + {}^{k}b_n \sin\omega_n x_1) =$$

$${}^{k}a_n \frac{e^{j\omega_n x_1} + e^{-j\omega_n x_1}}{2} + {}^{k}b_n \frac{e^{j\omega_n x_1} - e^{-j\omega_n x_1}}{2j} =$$

$$(1/2)\left({}^{k}a_n - j^{k}b_n \right) e^{j\omega_n x_1} + (1/2)\left({}^{k}a_n + j^{k}b_n \right) e^{-j\omega_n x_1}$$

These expressions, derived from Euler's equation, are inserted into the Fraunhofer equation as follows,

$$U(x_0) = \frac{e^{jkz} e^{j\frac{k}{2z}x_0^2}}{j\lambda z} \int_{-\infty}^{\infty} e^{-j\frac{2\pi}{\lambda z}x_0 x_1} dx_1 +$$

$$\frac{e^{jkz} e^{j\frac{k}{2z}x_0^2}}{j\lambda z} \left\{ \sum_{n=1}^{Bl} (1/2)\left({}^{k}a_n - j^{k}b_n \right) \int_{-\infty}^{\infty} e^{-j(\frac{2\pi}{\lambda z}x_0 - \omega_n)x_1} dx_1 + \sum_{n=1}^{Bl} (1/2)\left({}^{k}a_n + j^{k}b_n \right) \int_{-\infty}^{\infty} e^{-j(\frac{2\pi}{\lambda z}x_0 + \omega_n)x_1} dx_1 \right\}$$

This last equation can be simplified to,

$$U(x_o)=\frac{le^{jkz}e^{j\frac{k}{2z}x_0^2}}{j\lambda z}\left[\frac{\sin(\frac{\pi l}{\lambda z}x_0)}{\frac{\pi l}{\lambda z}x_0}\right]+$$

$$\frac{e^{jkz}e^{j\frac{k}{2z}x_0^2}}{j\lambda z}\sum_{n=1}^{Bl}\left\{(1/2)\left({}^{k}a_n-j^{k}b_n\right)l\left[\frac{\sin(\frac{\pi l}{\lambda z}x_0-\omega_n\frac{l}{2})}{\frac{\pi l}{\lambda z}x_0-\frac{\omega_n l}{2}}\right]+(1/2)\left({}^{k}a_n+j^{k}b_n\right)l\left[\frac{\sin(\frac{\pi l}{\lambda z}x_0+\omega_n\frac{l}{2})}{\frac{\pi l}{\lambda z}x_0+\frac{\omega_n l}{2}}\right]\right\}$$

This function contains three sinc terms ($\mathrm{sinc}(x)=x^{-1}\sin(x)$). In order to consider the effect of noise in the transmission function on the location of the first null, we, as a first step, analytically evaluate the location of the nulls for each of the sinc terms taken separately. The first sinc term,

$$\frac{le^{jkz}e^{j\frac{k}{2z}x_0^2}}{j\lambda z}\left[\frac{\sin(\frac{\pi l}{\lambda z}x_0)}{\frac{\pi l}{\lambda z}x_0}\right]$$

has nulls when the sin term equals $n\pi$. Thus there will be minimums when $x_0=\lambda zn/l$ for $n=1,2,3,.....$ The first positive minimum of the first sinc term will therefore be located at $x_0=\lambda z/l$.

The second sinc term,

$$(1/2)\left({}^{k}a_n-j^{k}b_n\right)l\left[\frac{\sin(\frac{\pi l}{\lambda z}x_0-\omega_n\frac{l}{2})}{\frac{\pi l}{\lambda z}x_0-\frac{\omega_n l}{2}}\right]$$

will have minimums when,

$$\frac{\pi l}{\lambda z}x_0-\omega_n\frac{l}{2}=n\pi$$

or,

$$x_0=\frac{\lambda zn}{l}+\frac{\lambda z\omega_n}{2\pi}$$

Previously we defined ω_n as

$$\omega_n=2\pi f_n,\quad f_n=n\Delta f=\frac{n}{l},\quad n=1,2,3,...$$

thus,

$$x_0 = \frac{\lambda z n}{l} + \frac{\lambda z}{2\pi}\frac{2\pi n}{l} = 2\frac{n\lambda z}{l}$$

This last expression tells us that the first nulls associated with the second sinc term are not located at the same places as the first null for the first sinc term. In fact, these nulls are twice as far from the origin of the axis system.

Similarly, for the third sinc terms the minimum will be located at,

$$\frac{\pi l}{\lambda z}x_0 + \omega_n \frac{l}{2} = n\pi$$

or,

$$x_0 = \frac{\lambda z n}{l} - \frac{\lambda z}{2\pi}\frac{2\pi n}{l} = 0$$

Thus, for the third sinc term, the first null is at the origin.

In summary, the three sinc terms have nulls at different places on the x-axis. Thus, the first null of the complex intensity function $U(x_0)$ is influenced by the noise in the transmission function $U(x_1)$. This finding leads to a consideration of the expectation of the intensity function $I(x_0)$. We will symbolize this expectation as $E\{I(x_0)\}$.

To compute the intensity function we must start with the complex amplitude. This is repeated below for reference.

$$U(x_o) = \frac{le^{jkz}e^{j\frac{k}{2z}x_0^2}}{j\lambda z}\left[\frac{\sin(\frac{\pi l}{\lambda z}x_0)}{\frac{\pi l}{\lambda z}x_0}\right] +$$

$$\frac{e^{jkz}e^{j\frac{k}{2z}x_0^2}}{j\lambda z}\sum_{n=1}^{Bl}\left\{(1/2)\left({}^{k}a_n - j^{k}b_n\right)l\left[\frac{\sin(\frac{\pi l}{\lambda z}x_0 - \omega_n\frac{l}{2})}{\frac{\pi l}{\lambda z}x_0 - \frac{\omega_n l}{2}}\right] + (1/2)\left({}^{k}a_n + j^{k}b_n\right)l\left[\frac{\sin(\frac{\pi l}{\lambda z}x_0 + \omega_n\frac{l}{2})}{\frac{\pi l}{\lambda z}x_0 + \frac{\omega_n l}{2}}\right]\right\}$$

This complex amplitude can be represented simply as

$$U(x_o) = M + \eta$$

In this expression, M is the complex amplitude that occurs in the absence of noise, and, η is a complex valued term dependent on the presence of noise.

We immediately obtain,

$$|U(x_0)|^2 = |M|^2 + 2\mathrm{Re}(M\overline{\eta}) + |\eta|^2$$

In this last expression, $|M|^2$ is the intensity profile $I(x_0)$ we have discussed above. The term $2\mathrm{Re}(M\overline{\eta})$ has the form

$$2\mathrm{Re}(M\overline{\eta}) = \frac{l^2}{\lambda^2 z^2}\frac{\sin(\frac{\pi l}{\lambda z}x_o)}{(\frac{\pi l}{\lambda z}x_o)}\sum_{n=1}^{Bl}({}^k a_n)\left[\frac{\sin(\frac{\pi l}{\lambda z}x_0 - \omega_n\frac{l}{2})}{(\frac{\pi l}{\lambda z}x_0 - \omega_n\frac{l}{2})} + \frac{\sin(\frac{\pi l}{\lambda z}x_0 + \omega_n\frac{l}{2})}{(\frac{\pi l}{\lambda z}x_0 + \omega_n\frac{l}{2})}\right]$$

Immediately observe that this term, $2\mathrm{Re}(M\overline{\eta})$, takes the value zero in expectation. That is $E\{2\mathrm{Re}(M\overline{\eta})\} = 0$.

The term $|\eta|^2$ simplifies to

$$|\eta|^2 = \frac{l^2}{\lambda^2 z^2}\left(\sum_{n=1}^{Bl}\frac{1}{2}({}^k a_n)P\right)^2 + \frac{l^2}{\lambda^2 z^2}\left(\sum_{n=1}^{Bl}\frac{1}{2}({}^k b_n)Q\right)^2$$

where

$$P = \left[\frac{\sin(\frac{\pi l}{\lambda z}x_0 - \omega_n\frac{l}{2})}{(\frac{\pi l}{\lambda z}x_0 - \omega_n\frac{l}{2})} + \frac{\sin(\frac{\pi l}{\lambda z}x_0 + \omega_n\frac{l}{2})}{(\frac{\pi l}{\lambda z}x_0 + \omega_n\frac{l}{2})}\right]$$

$$Q = \left[\frac{\sin(\frac{\pi l}{\lambda z}x_0 - \omega_n\frac{l}{2})}{(\frac{\pi l}{\lambda z}x_0 - \omega_n\frac{l}{2})} - \frac{\sin(\frac{\pi l}{\lambda z}x_0 + \omega_n\frac{l}{2})}{(\frac{\pi l}{\lambda z}x_0 + \omega_n\frac{l}{2})}\right]$$

The value of $|\eta|^2$ in expectation can be seen to depend solely on the variances of the noise coefficients ${}^k a_n$ and ${}^k b_n$ since the cross-product terms will drop out.

To summarize our results concerning signal intensity and transmission noise, the signal intensity in the presence of noise should be the sum of the deterministic intensity profile $I(x_0)$ plus two stochastic terms. One of the stochastic terms converges with larger sample size to zero, the second will grow with noise intensity in expectation. We now turn to numerical experiments to examine these predictions.

Numerical Methods

In the theory section above, we have shown that the presence of a stochastic transmission filter in the aperture leads to a perturbation of the intensity profile. This perturbation is predicted to grow with the variance of the noise.

We also demonstrated in the theory section that the first null or minimum in the intensity profile contains information about the frequency of the field penetrating the aperture, and contains information about the aperture size. Our goal, as stated in the introduction, is to understand the influence of noise on the measurement of the first null.

We have computed the intensity profile in the setting of noise by using the Rice representation of transmission noise in the equation for the complex propagated amplitude. We computed individual realizations of the intensity profiles and then averaged across relatively large sample sizes (N=500). We have evaluated, in this way, the impact of transmission noise on estimation of the first null.

Thus, prior to showing results of the study, we will discuss how we developed transmission noise using the Rice representation, and we will discuss the technique we have used to estimate the first null. This technique employs Legendre polynomials.

The Rice Representation

The Rice white noise is generated by multiplying sine and cosine waves by independently distributed normal random variables. The sine and cosine waves in our case represent spatial frequency not temporal frequency as more commonly encountered. The equation we have used for the noise is

$$\eta(x_1) = \gamma \sum_{n=1}^{Bl} \left({}^{k}a_n \cos \omega_n x_1 + {}^{k}b_n \sin \omega_n x_1 \right).$$

In this equation for the Rice noise we have added a multiplication factor γ so that the noise variance can be scaled. We do this because in presenting our results, we will use variance as the independent variable.

We computed the variance of η in the following manner. The coefficients ${}^{k}a_n$ and ${}^{k}b_n$ were drawn using a zero mean variance one random number generator embedded in MATLAB version 5.3 (the command "randn"). The variance of η was computed by averaging over one hundred draws of random coefficients and by averaging over one thousand spatial points. Thus the variance we report applies across the entire aperture. The bandwidth product Bl used, which determines the number of spatial frequencies in our Rice representation was initially taken as fifty. Various multiplication factors were put in the Rice white noise generator subprogram (MATLAB version 5.3 and called "var_det.m"). Results for different values of the multiplication factor γ are tabulated in table1.

Multiplication Factor	Variance
0.025	0.031
0.050	0.124
0.075	0.287
0.100	0.508
0.125	0.786
0.150	1.13

Table I. Within aperture variance as a function of multiplication factor used before the Rice representation. One hundred statistical realizations used and one thousand spatial points sampled. Fifty spatial frequencies considered.

Variance as a function of the multiplication factor γ is plotted in Figure 1. The resulting curve is not a straight line but is linearized by logarithmic transformation of both variables. This linearization is shown in Figure 2 below. Linearization with a log-log transformation indicates that the functional relationship is a power law. Fitting the log-log transformed data provides

$$\text{var} \propto \gamma^n$$

and n was found to be 2.0091614, as expected.

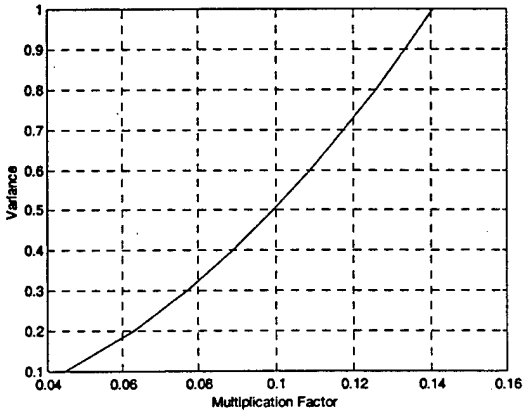

Figure 1. A plot of the variance of the Rice representation as a function of the multiplication factor γ.

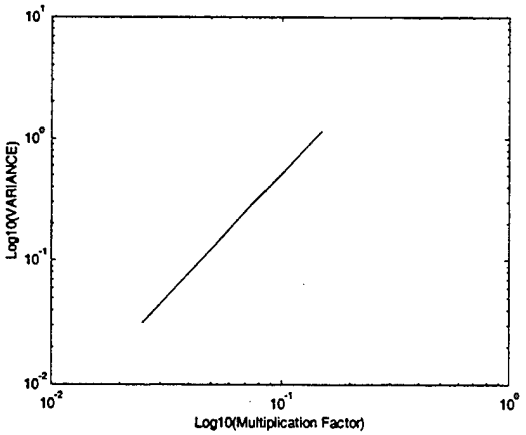

Figure 2. A plot of the variance of the Rice representation as a function of the multiplication factor γ with both factors transformed using logarithms to the base ten.

This power law relationship has been tested to a maximum value of 0.8 for the multiplication factor and has been noted to be correct well within numerical experiment error.

Legendre Polynomial Curve Fitting

A number of methods to determine the location of the maximum and minimum points of the diffraction pattern were evaluated. The Legendre Polynomial method of curve fitting seemed to be the most accurate method.

One of the advantages of the Legendre Polynomial method over the other methods was that it gave the smoothest curve and truest fitting curve when the diffraction pattern was noisy. In addition, through the use of recursive equations, the first derivative of the fitted curve could be determined. By setting the first derivative to zero, the locations of the maximum and minimums of the diffraction pattern could be analytically calculated.

The Legendre polynomial method has certain limitations. The first one is that with the standard polynomial formula, the x-axis needs to be evaluated between negative one to one. In our program, the axis is fitted to the actual data through change of variables on the x-axis. Care must be used in determining the number of polynomial terms used. If too few terms are used, the equation will not be flexible enough to obtain a good fit. However too many terms will greatly increase computation time and could induce round off errors. Seventy-five terms were used in our program. After the change of variable was accomplished the x-axis was divided into 10000 segments. This resulted in increased resolution.

Another limitation with Legrendre polynomials is that diffraction curves containing too many peaks and depressions are fitted accurately only after special attention. This restriction can be overcome by either selecting an aperture and image domain value that would minimize the number of peaks and valleys needing fitting, or by evaluating just the center portion of the diffraction pattern. In our program the aperture size was 1 meter and the image domain was limited to 50 meters.

We fitted Legendre polynomials to our simulation data using a technique described in G. J. Borse's book, "Numerical Methods with Matlab" [9]. The scheme behind this method is described in the following.

The fundamental problem is to fit a function $f(x)$ that is known at the points $x_1, x_2, x_3 ..... x_N$ to a finite sum of Legendre polynomials. That is we seek coefficients $a_i, i = 1,2,3,.....N$ such that

$$y = f(x) = \sum_{k=0}^{N} a_{N-k+1} P_k(x)$$

The needed coefficients are found using the method of least squares. In this method a sum of squares of deviations is formed and those coefficients that minimize this sum of squares of deviations are determined using partial differentiation and solving the resulting linear set of equations. In MATLAB this operation is done somewhat automatically using the backslash command "\". In the program to perform the least squares fit, one creates the Vandermonde matrix and solves for the coefficients as shown below.

$$M = \begin{bmatrix} f_1(x_1) & f_2(x_1) & \cdots & f_{n-1}(x_1) & f_n(x_1) \\ f_1(x_2) & f_2(x_2) & \cdots & f_{n-1}(x_2) & f_n(x_2) \\ \vdots & \vdots & \ddots & \vdots & \vdots \\ f_1(x_N) & f_2(x_N) & \cdots & f_{n-1}(x_N) & f_n(x_N) \end{bmatrix}$$

$$a = M \setminus y$$

Once the coefficients of the Legrendre polynomials are calculated, the locations of the maximums and minimums in the data can be estimated.

The location of the maximums and minimums are computed by taking the first derivative of the fitted curve. Taking the derivative of

$$y = f(x) = \sum_{k=0}^{N} a_{N-k+1} P_k(x)$$

as a function of x is simplified through the use of known recursion relationships for Legendre polynomials. Specifically

$$P_0'(x) = 0$$
$$P_1'(x) = 1$$
$$P_{n+1}' = (n+1)P_n(x) + P_n'(x)$$

The maximum and minimum locations were obtained by finding the points at which the first derivative is equal to zero. We actually accomplished this in a two step process. We obtained a first estimate of maxima and minima location by determining the locations where the first derivative curve sign changed. These values were then entered into the subroutine first_derv_L2 that calculated more accurately the location of the first derivative zeros using the bisection method.

Results

Effect of Noise in the Aperture.

Various levels of white noise were added to the aperture. Variance at any given point was used in order to characterize the level of noise in the aperture. The bandwidth for the results in this section was taken as 50.

During a run, the variance of the aperture transmission function was calculated as a check on the prior observations and calibration shown in Figure 1. The mean variance was then obtained as the mean of the individual variances in each of the five hundred runs at a specific noise level. This mean variance is the independent variable (x-axis) in the following graphs. The first minimum positions are graphed on the y-axis.

An interesting relationship is observed when comparing diffraction pattern null (minimum) locations to the level of input variance. As seen in Figure #3, the mean first minimum locations (that provide us our frequency or wavelength estimate) appear robust to the presence of noise. There is only a slight outward movement of the null as variance is increased. However our estimate of the null location degrades markedly with increased transmission noise in the aperture as is seen by the increasing length of the bars on the graphs which represent three times the standard deviation.

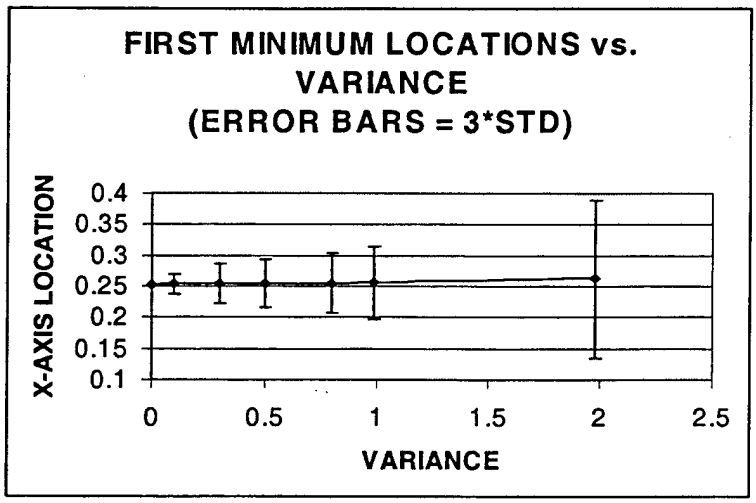

Figure 3. A plot of the location of the first minimum as a function of variance.

Effect of Bandwidth on the Diffraction Pattern.

The bandwidth of the input white noise defining the transmission screen also effects the diffraction pattern. Examining the Rice representation one postulates that the transmission screen variance would increase with bandwidth. In fact, a direct linear relationship was found between bandwidth and variance. Specifically, if y is the variance and x is the bandwidth, we found

$$y = 0.000980 + 0.0099098x$$

with the multiplication factor γ of 0.0995. The standard error of the fit was 0.008114 and the coefficient of determination (r^2) was 0.9999979. The standard error of the fit is defined as the standard deviation of the calibration points from the curve fit. Likewise r^2 is defined as

$$r^2 = \frac{Sum\,of\ Squares\,Explained\,by\,Regression}{Total\,Sum\,of\ Squares(Before\,Regression)}$$

The multiplication factor of 0.0995 (number multiplying random number term to produce the coefficient for the cosine and sine terms of the rice white noise) will produce a variance in the input aperture of 0.498, when the bandwidth was 1:50 as can be seen in Figure 1 where 50 spectral bands were used. When the bandwidth was reduced by a factor of ten from 1:50 to 1:5, the variance of the input aperture was also reduced by a factor of ten from 0.498 to 0.0498. This reduction is expected given the form of the above shown regression equation.

For a relatively broad selection of bandwidths, transmission filter variance has been shown to be a linear function of bandwidth. This relationship is shown in Figure #4.

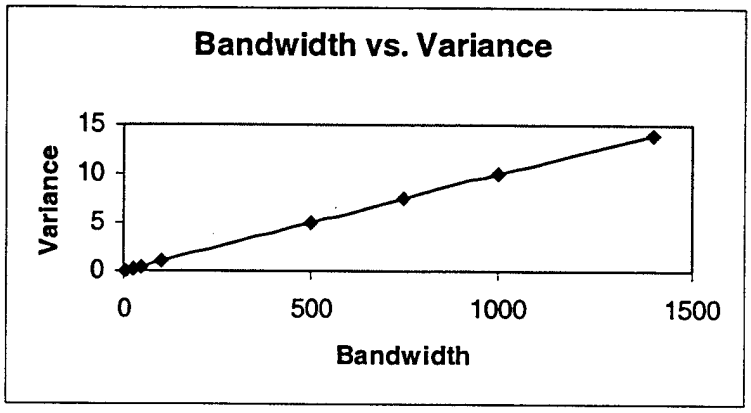

Figure 4. Direct linear relationship between bandwidth and variance.

As is seen in Figure #5, relatively large increases in bandwidth have a small effect on the estimate of the position of the first diffraction pattern null. Interestingly, the variability of that estimate is also effectively independent of bandwidth increases until a bandwidth of 1000 is reached.

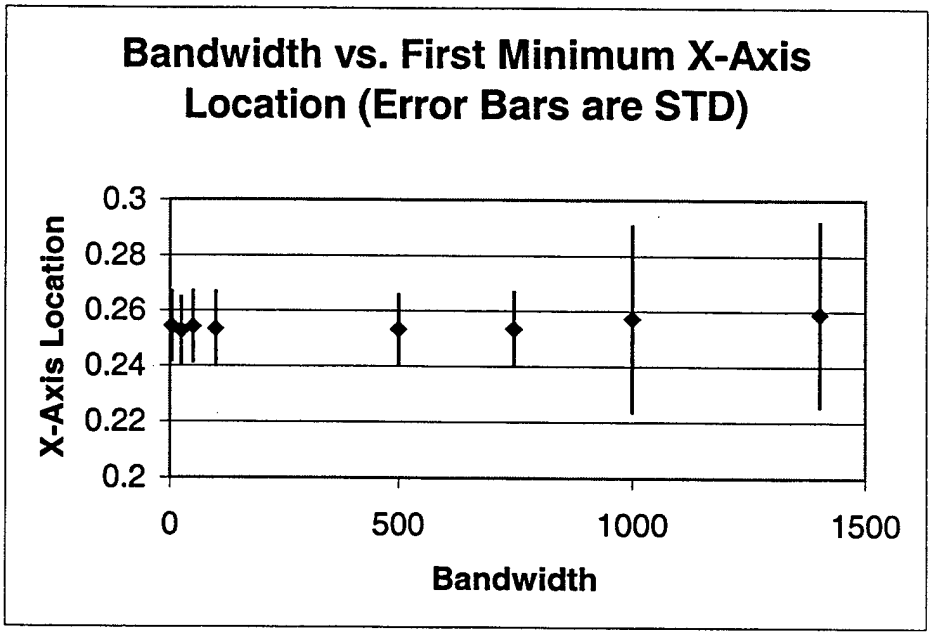

Figure 5. The effect of bandwidth on the estimates of the x-axis location of the first minimum. Bars show ± three standard deviations.

Thus, at a fixed bandwidth increasing the transmission filter variance by increasing the amplitude of the transmission filter slightly shifts the estimate of the first null while increasing the variance of that estimate. On the other hand, increasing the bandwidth and

thereby increasing the filter variance has a lesser effect on the estimate of the first null. We will seek to understand this finding more deeply in subsequent research.

Statistics Used in Results Evaluation

The program was run 500 times at each noise variance level. All variables were cleared between each run. A method was needed to evaluate the validity of the estimated of the first nulls or first minimum points.

The first part of this method was to evaluate if the subprogram, which calculated the Rice white noise, was actually producing white noise of a specific bandwidth. A program called test_rice accomplished this task. Using the Rice algorithm, white noise was first generated and then evaluated to determine if it has a normal distribution and secondly its fast Fourier transform (FFT) was taken to determine the extent of its bandwidth.

Since the white noise generated via the Rice algorithm has a normal distribution, it was felt that the x axis location of the diffraction pattern nulls might not necessarily exhibit a normal distribution. To determine if this was occurring, the mean, standard deviation, skewness (third moment) and kurtosis (fourth moment) were calculated. The standard deviation (σ), of course, determines the overall spread of the data. With normally distributed data skewness (the third moment) is equal to zero. Finally, kurtosis evaluates if the data is distributed either excessively flat (platykurtic) or excessively steep (leptokurtic). If the data are distributed in terms of the normal distribution, the kurtosis equals 3.0. If kurtosis is greater than 3.0 the distribution will have a peaked form.

The two graphs below show that for bandwidths up to 500, the 3^{rd} and 4^{th} moments of the null estimates are essentially invariant. The skewness and kurtosis are not zero, as would occur were the distribution normal or Gaussian.

CONCLUSION

This report is an initial study of apertures and errors that may be associated with the use of apertures in the measurement of material properties.

The setting for this article is a situation wherein scattered radiation is received from a scene and one wishes to determine amplitudes at various frequencies. From these

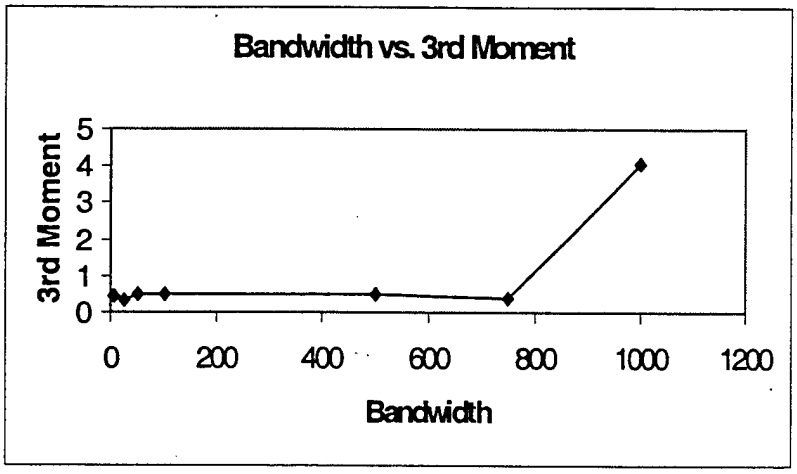

Figure 6. The effect of bandwidth on the skewness (3rd moment) of the distribution of the first minimum estimates.

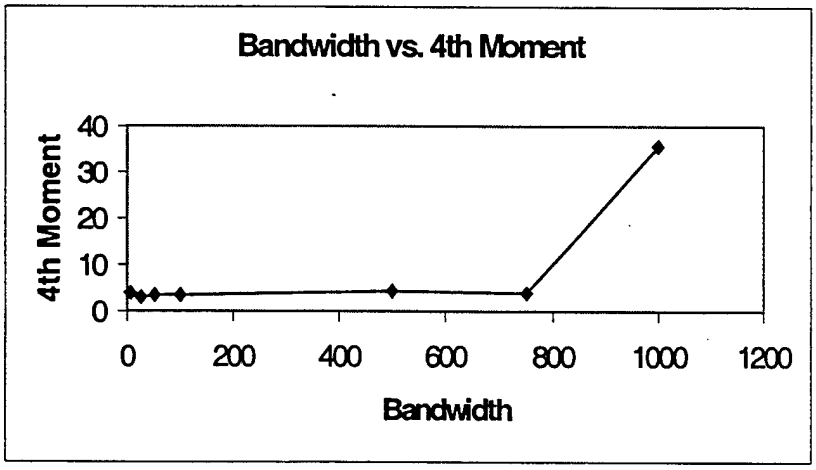

Figure 7. The effect of bandwidth on the kurtosis (4th moment) of the distribution of the first minimum estimates.

amplitudes, and possibly phase data, material dielectric constant and conductivity can be determined and the material identified. This work is thus pursued in the context of an inverse problem.

We have used an aperture to diffract the returning signal for the purpose of frequency estimation and we have used the first null in the diffraction pattern as an estimate (the position of the first null is directly proportional to the wavelength).

In performing this study we recognize that any aperture that might be used would be imperfect and we represented these imperfections by applying band limited Gaussian noise to the aperture transmission function.

We have found that the mean location of the diffraction pattern first minimum only slightly increases with respect to increasing variance of the band limited noise in the input aperture (bandwidth held constant). However the standard deviation of the first null estimate increases dramatically as noise variance increases.

Holding bandwidth constant, we increased transmission filter noise variance by increasing amplitude. As reported above, we found that the mean position of the first null was left largely unchanged while the quality of the estimator degraded. We also increased the variance of the transmission filter by increasing the noise bandwidth. In this case, we found that the mean position of the first null remained relatively constant over a broad band with an apparent slower degradation of null estimate quality.

In summary, estimating wavelength or frequency, using the first null of a diffraction pattern, seems robust with respect to mean value in the presence of aperture noise. Bandwidth and noise point-wise variance appear to have somewhat independent influences on the quality of the estimate.

This use of the first diffraction null is not as sensitive to noise as were the measurements reported in [3,4]. However, the measurements in these references, while being made in a materials estimation setting, involved different variables. Specifically, in [4] the variable of interest was the ratio of complex amplitudes. The work in this report illustrates that measurements made in an inverse setting are not necessarily vulnerable to noise in the device.

The reader should note that the aperture study we have performed is applicable to the situation of a uniformly excited antenna. The diffraction pattern we have analyzed is that which would be produced by such a system. One can infer from our results that the main beam of such an antenna would be robust to random errors in surface excitation.

REFERENCES

1. J. Stratton, Electromagnetic Theory, pp.321-325, McGraw-Hill (1941).
2. D. Colton and R. Kress, Inverse Acoustic and Electromagnetic Scattering Theory, Springer-Verlag (1998).
3. R. Beezeley and R. Krueger, "An Electromagnetic Inverse Problem for Dispersive Media", J. Math. Phys., 26, 317, (1985).
4. R. Albanese, R. Medina, J Penn: "An Electromagnetic Inverse Problem in Medical Science in Inverse Problems and Invariant Imbedding, edited by Corones, Kristensson, Nelson and Seth, Society for Industrial and Applied Mathematics, (1992
5. J.Goodman, Introduction to Fourier Optics, pp.57-75, McGraw-Hill (1968).
6. G.R. Fowles, Introduction to Modern Optics, 2nd edition, Holt, Rinehart, and Wilson (1975)

7. L. Chu, "Physical Limitations of Omni-Directional Antennas," J. Appl. Phys, 19, 1163, (1948).
8. J. Bendat, Principles and Applications of Random Noise Theory, John Wiley & Sons, 1958.
9. G. Borse, Numerical Methods with Matlab, pp.324-331,PWS Publishing Co. (1997).